Title

Exploring New Assembly Modes of Uranyl Terephthalate: Templated Syntheses and Structural Regulation of a Series of Rare 2D → 3D Polycatenated Frameworks

Journal

Inorganic Chemistry, 56(14)

ISSN

0020-1669

Authors

Mei, Lei
Wang, Cong-zhi
Zhu, Liu-zheng
et al.

Publication Date

2017-07-17

DOI

10.1021/acs.inorgchem.7b00312

NOT FINAL PUBLISHED VERSION

Exploring New Assembly Modes of Uranyl Terephthalate: Templated Syntheses and Structural Regulation of a Series of Rare 2D → 3D Polycatenated Frameworks

Lei Mei,[†] Cong-zhi Wang,[†] Liu-zheng Zhu,[†] Zeng-qiang Gao,[&] Zhi-fang Chai,[†,‡] and Wei-qun Shi[,†]*

[†] Laboratory of Nuclear Energy Chemistry, Institute of High Energy Physics, Chinese Academy of Sciences, Beijing 100049,China

[&] Beijing Synchrotron Radiation Facility, Institute of High Energy Physics, Chinese Academy of Sciences, Beijing 100049, China

[‡] School of Radiological and Interdisciplinary Sciences and Collaborative Innovation Center of Radiation Medicine of Jiangsu Higher Education Institutions, Soochow University, Suzhou 215123, China

Keywords: Actinide • Uranyl-organic compound • Polycatenated • Templated Synthesis • pH-regulated

Abstract: The reaction of uranyl nitrate with terephthalic acid (**H_2TP**) under hydrothermal conditions in the presence of an organic base, 1,3-(4,4‘-bispyridyl)propane (**BPP)** or 4,4‘-bipyridine (**BPY**), provided four uranyl terephthalate compounds with different entangled strcutures by a pH-tuning method. $[UO_2(\mathbf{TP})_{1.5}](H_2\mathbf{BPP})_{0.5}$ (**1**) obtained in relatively acidic solution (final aqueous pH, 4.28) crystallizes in the form of a non-interpenetrated honeycomb-like 2D network structure. An elevation of the solution pH (final pH, 5.21) promotes the formation of a dimeric uranyl-mediated polycatenated framework, $[(UO_2)_2(\mu\text{-}OH)_2(\mathbf{TP})_2]_2(H_2\mathbf{BPP})_2$ (**2**). Another new polycatenated framework with a monomeric uranyl unit, $[(UO_2)_2(\mathbf{TP})_3](H_2\mathbf{BPP})$ (**3**), begins to emerge as a minor accompanying product of **2** when the pH is increased up to 6.61, and turn out to be a significant product at pH 7.00. When more rigid but small-size **BPY** molecules replace **BPP** molecules, $[UO_2(\mathbf{TP})_{1.5}](H_2\mathbf{BPP})_{0.5}$ (**4**) with a polycatenated framework similar to **3** was obtained in a relatively acidic solution (final pH, 4.81). The successful preparation of **2**, **3** and **4** represents the first report of uranyl-organic polycatenated frameworks derived from a simple terephthalic acid linker. A direct comparison between these polycatenated frameworks and previously reported uranyl terephthalate compounds suggests that the template and cavity-filling effects of organic bases (such as **BPP** or **BPY**), in combination with specific hydrothermal conditions, promote the formation of uranyl terephthalate polycatenated frameworks.

■ INTRODUCTION

Actinide-bearing hybrid materials, especially actinide coordination compounds, have drawn much attention from chemists and material scientists, and considerable research efforts have been devoted to this field due to its relevance to nuclear waste management, as well as the intriguing 5*f* bonding features of actinide elements.[1-8] As one of the most extensively studied actinides, uranium is incorporated in numerous actinide-organic coordination polymers in two oxidation states, U(VI)[9-11] and U(IV).[12-14] Compared to oxygen-sensitive U(IV), U(VI), which occurs primarily as the linear uranyl cation ($[UO_2]^{2+}$), is stable under ambient atmosphere and has accordingly been studied more extensively. The inactive terminal oxo groups of uranyl often prevent axial bonding interactions, resulting in any further coordination occurring in the equatorial plane. As a result, uranyl-organic coordination polymers usually prefer to form one-dimensional (1D) chains,[10, 15-17] or two-dimensional (2D) sheets, [18-24] rather than three-dimensional (3D) frameworks that require structural connectivity in the third axial dimension.[25-32]

2D networks or 3D frameworks with large cavities or pores can readily achieve a high degree of self-assembly by an entangled mode in the solid state, and thus afford a variety of intriguing topological structures as well as fascinating properties.[33-35] Generally, the different types of entangled systems that have been reported can be classified as interpenetrated, polycatenated (parallel or inclined), or Borromean-linked arrays depending on the assembly patterns.[33] Polycatenation essentially always promotes an increase in the dimensionality of the final assemblies in comparison with the dimensionality of the basic building motifs, whereas there is generally no change in dimensionality for the interpenetration or Borromean-type assembly modes.[36] This is also the case for uranyl-organic compounds, especially those in 2D networks,

which can assemble in similar entangled patterns. For example, several uranyl-based cases including parallel 2D + 2D → 2D interpenetration have been reported.[19, 24, 29, 37-41] In comparison to a relatively large number of uranyl-organic compounds exhibiting parallel interpenetration, polycatenatenation remains rare for uranyl-organic compounds.[42-45] The first case of polycatenatenated uranyl-organic compound, reported by Cahill in 2006, was assembled from mixed ligands of bipyridine and adipic acid through inclined polycatenatenation of three sets of 2D networks.[42] More recently, Wang et al. reported another uranyl-organic polycatenated framework derived from 3,5-di(4-carboxylphenyl) benzoic acid, an aromatic tricarboxylic acid.[43] This unique structure exhibits high radiation and chemical stability, as well as the potential for selectively removing cesium from aqueous solutions, which emphasizes the intriguing properties of actinide polycatenated structures. Soon afterwards, Thuéry et al. prepared two 2D + 2D → 3D uranyl-organic polycatenated frameworks via dicarboxylic acids (4,4‘-biphenyldicarboxylic acid[44] or 2,5-thiophenedicarboxylic acid[45]) using $[Ni(bipy)_3]^{2+}$ or $[Ag(bipy)_2]^{+}$ counter ions as the templating agent. Besides inclined polycatenatenation in the uranyl-organic coordination polymers, Thuéry et al have recently reported an interesting case of parallel polycatenatenation,[46] which gave a 2D + 2D → 3D framework induced by a flexible pimelate. The third type of entanglement, a Borromean-type array, has also been achieved in uranyl-based compounds by the same group utilizing long-chain aliphatic dicarboxylates.[47]

Herein, we report the preparation of novel uranyl-organic polycatenated frameworks from a relatively simple organic ligand, terephthalic acid (**H_2TP**). Although uranyl terephthalate (**TP**) compounds, or similar derivatives, have been previously repoted, they include only parallel interpenetration[38-39] or non-interpenetration[23, 31-32, 39, 48-53] modes, not uranyl-organic polycatenated frameworks. Previous results for uranyl-organic (inclined) polycatenated

frameworks by Cahill, Wang and Thuéry indicate that the large pore sizes (such as square or hexagonal) in the relatively rigid 2D networks with are prone to promote the inclined 2D→3D polycatenation. A preliminary comparison between previouly-reported uranyl polycatenated frameworks and uranyl terephthalate network (Scheme 1) reveals that, the grid size of the uranyl terephthalate system (22.7 Å*17.8 Å)[39] is smaller than that of the uranyl/4,4'-biphenyldicarboxylic acid system (32.4 Å* 22.8 Å),[44] but larger than that of the uranyl/3,5-di(4-carboxylphenyl) benzoic acid system (17.2 Å*11.2 Å).[43] The modest grid size of the uranyl terephthalate system presents the possibility of assembly via an inclined polycatenated mode. Therefore, it is reasonable to speculate that, when the grid size of a 2D network is sufficiently large, polycatenated assembly of 2D networks in a pattern of inclined polycatenatenation might occur under favorable conditions. We have succeeded in the assembly of uranyl-terephthalate polycatenated frameworks through a templated-synthsis method by using organic bases, 1,3-(4,4'-bispyridyl)propane (**BPP)** or 4,4'-bipyridine (**BPY**) (Scheme 2), as the template agent under hydrothermal conditions. Interestingly, it has been also found that alteration of the pH or changing the template agent can dramatically affect hydrothermal processes, resulting in a series of new uranyl-terephthalate polycatenated frameworks. The structural evolution, as well as possible reaction mechanisms are proposed, and DFT calculations were conducted to explore the bonding features of the synthesized uranyl compounds.

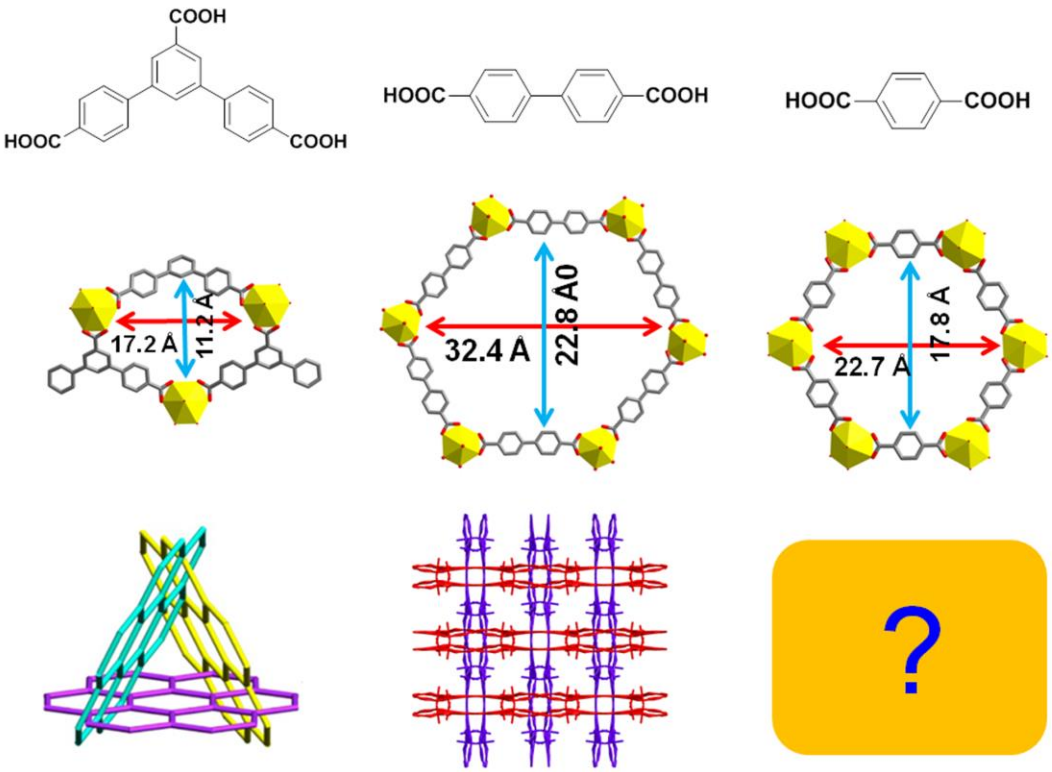

Scheme 1. A preliminary comparison between previouly-reported uranyl polycatenated frameworks and the uranyl terephthalate network. Left: uranyl/3,5-di(4-carboxylphenyl) benzoic acid system;[43] Middle: uranyl/4,4'-biphenyldicarboxylic acid system;[44] Right: uranyl terephthalate system.[39]

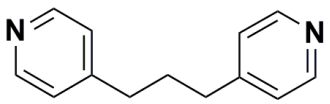

1,3-(4,4'-bispyridyl)propane (**BPP**)

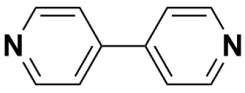

4,4'-bipyridine (**BPY**)

Scheme 2. Two types of organic bases, 1,3-(4,4'-bispyridyl)propane (**BPP**) and 4,4'-bipyridine (**BPY**), used as the templating agents in this work.

■ EXPERIMENTAL SECTION

Materials and Methods. *Caution! Due to the radioactive and chemically toxic nature of uranyl nitrate hexahydrate, $UO_2(NO_3)_2{\cdot}6H_2O$, suitable precautions for safety and protection must be taken.* The following reactants were used in the synthesis: uranyl nitrate hexahydrate ($UO_2(NO_3)_2{\cdot}6H_2O$, Sinopharm Chemical Reagent, 99%), terephthalic acid (**H_2TP**, Sinopharm Chemical Reagent, 99%), 1,3-di(4-pyridyl)propane (**BPP**, Acros, 98%), 4,4'-bipyridine (**BPY**, Aladdin, 98%), ultrapure water (resistivity of 18.2 $M\Omega{\cdot}cm^{-1}$). All commercially supplied chemical reagents were used without further purification.

Powder X-ray diffraction measurements (PXRD) were made using a Bruker D8 Advance diffractometer with Cu Kα radiation (λ = 1.5406 Å) in the range 5-50° (step size: 0.02º). Thermogravimetric analysis (TGA) was performed on a TA Q500 analyzer over the temperature range of 25-600 °C in air atmosphere with a heating rate of 5 °C per minute. The fluorescence spectra were measured on a Hitachi F-4600 fluorescence spectrophotometer equipped with a xenon lamp and solid sample holder under excitation at a wavelength of 420 nm,[54] which is suitable for uranyl excitation. The photomultiplier tube voltage was 500V, the excitation and the emission slit width were both 5.0 nm, and the scan speed was 60 nm per minute.

Synthesis. All the uranyl compounds in this work were hydrothermally synthesized under autogenous pressure using 15 ml Teflon-lined Parr type autoclaves.

$[UO_2(TP)_{1.5}](H_2BPP)_{0.5}$ (1). $UO_2(NO_3)_2{\cdot}6H_2O$ (0.50 M, 0.20 ml), **H_2TP** (34.0 mg, 0.20 mmol), **BPP** (31.0 mg, 0.18 mmol), NaOH (4.0 mg, 0.10 mmol), ultrapure water (5.0 ml) was loaded into a 15 ml autoclave. The autoclave was sealed and heated to 180 °C in an oven for 3 days, then cooled to ambient temperature. The final pH of the aqueous solution was 4.59. Dark yellow crystals of compound **1** accompanied by small-size brown crystals were produced; the

yellow crystals were filtered off, rinsed with ultrapure water and ethanol, and subjected to air-drying at room temperature.

$[(UO_2)_2(\mu\text{-}OH)_2(TP)_2]_2(H_2BPP)_2$ (2). $UO_2(NO_3)_2{\cdot}6H_2O$ (0.50 M, 0.20 ml), **H_2TP** (34.0 mg, 0.20 mmol), **BPP** (31.0 mg, 0.18 mmol), NaOH (10.0 mg, 0.25 mmol), ultrapure water (5.0 ml) were loaded into a 15 ml autoclave. The autoclave was sealed and heated to 180 °C in an oven for 3 days, then cooled to ambient temperature. The final pH of aqueous solution was 5.71. Luminous yellow block crystals of compound **2** accompanied by small amount of unknown brown crystals were produced; the yellow crystals were filtered off, washed with ultrapure water and ethanol, and subjected to air-drying at room temperature. Yield: 12.4 mg, 12 % based on uranium.

$[(UO_2)_2(TP)_3](H_2BPP)$ (3). $UO_2(NO_3)_2{\cdot}6H_2O$ (0.50 M, 0.20 ml), **H_2TP** (34.0 mg, 0.20 mmol), **BPP** (31.0 mg, 0.18 mmol), NaOH (16.0 mg, 0.40 mmol), ultrapure water (5.0 ml) were loaded into a 15 mL autoclave. The autoclave was sealed and heated to 180 °C in an oven for 3 days, then cooled to ambient temperature. The final pH of aqueous solution was 7.00. A mixture of small yellow crystals of compound **2** and brown crystals of compound **3,** accompanied by unidentified microcrystals or powder were produced the compounds of interest were filtered off, washed with ultrapure water and ethanol, and subjected to air-drying at room temperature.

$[UO_2(TP)_{1.5}](H_2BPY)_{0.5}$ (4). $UO_2(NO_3)_2{\cdot}6H_2O$ (0.50 M, 0.20 ml), **H_2TP** (34.0 mg, 0.20 mmol), **BPY** (30.0 mg, 0.20 mmol), NaOH (4.0 mg, 0.10 mmol), ultrapure water (5.0 ml) were loaded into a 15 ml autoclave. The autoclave was sealed and heated to 180 °C in an oven for 3 days, then cooled to ambient temperature. The final pH of aqueous solution was 4.81. Yellow crystals of complex **4**, accompanied by a considerable amount of small-size orange crystals, were

produced; the yellow crystals were filtered off, washed with ultrapure water and ethanol, and subjected to air-drying at room temperature.

Control experiments without any organic bases added: In order to explore the role of organic base, **BPP** or **BPY**, in the formation of uranyl terephthalate polycatenated frameworks, a set of similar hydrothermal reactions using $UO_2(NO_3)_2 \cdot 6H_2O$ and **H_2TP** in the absence of any organic base were conducted with different amounts of NaOH solution added. This procedure yielded only transparent stick crystals of **H_2TP** at lower pH, or at higher pH light yellow microcrystal that could not be characterized.

X-ray Single Crystal Structure Determination. X-ray diffraction data for compounds **1**, **3** and **4** were all collected on a Agilent SuperNova X-ray CCD diffractometer with a Cu Kα X-ray source (λ = 1.54178 Å) at 150.01(10) K, 294.82(10) K, and 278(5) K, respectively. Standard Agilent Crysalis software was used for the determination of the unit cells and data collection control. X-ray diffraction data for compound **2** was acquired using a Bruker D8 VENTURE X-ray CMOS diffractometer with a Cu Kα X-ray source (λ = 1.54178 Å) at 170(2) K. Using Olex2,[55] all crystal structures were solved by means of direct methods (SHELXS-97[56]) and refined with full-matrix least squares on SHELXL-2014.[56-57] All non-hydrogen atoms were refined with anisotropic displacement parameters. The carbon-bound hydrogen atoms were placed at calculated positions and all hydrogen atoms were treated as riding atoms with an isotropic displacement parameter equal to 1.2 times that of the parent atom. The structure of **2** was treated as a non-merohedral twin, where a HKLF5 file was generated with TwinRotMat/PLATON, and the code HKLF 5 in combination with BASF was used to extend the SHELXL refinement. Refinement of the twin components in **2** converged at 0.853(3): 0.147(3). Moreover, the non-centrosymmetric structure of **3** or **4** appeared to be a racemic twin, which was

modeled using both the TWIN and BASF procedures. Refinement of the twin components ultimately converged at 0.432(13): 0.568(13) for **3**, and 0.56(2): 0.44(2) for **4**. The use of a DFIX (O-U, O-C) restraint was necessary to create a chemically sensible model for **4**; SIMU and ISOR were used to constrain the displacement parameters of the phenyl and pyridyl groups and even out the electron density associated with disordered portions of the moieties for both **2** and **4**. For all four compounds, the solvent molecules as well as (part of) the organic-base cations in the structure are highly disordered and impossible to be modeled as discrete atomic sites. To resolve this issue, the contribution of solvent-electron density was removed using the SQUEEZE/PLATON procedure,[58] thereby producing a set of solvent-free diffraction intensities used for improving the structure refinements. Specially, for the twining cases of **2**, **3** and **4**, the use of SQUEEZE/PLATON was based on the detwinning option in SHELXL2014, where a twin.cif and twin.fcf ('LIST 8'type) from a converged SHELXL twining refinement job (based on twin.ins including BASF/HKLF5 or BASF/TWIN records) serve as the input files.[59] It should be mentioned that poor diffraction resulting from small dimensions, as well as the presence of twinning, lead to relatively high R_1 and wR_2 values for **2** and **4**. The final formula for compound **2** was calculated from the crystallographic results in combination with elemental analyses and TGA, while those for compounds **1**, **3**, and **4**, were referenced to that of **2**, as well as considering charge balance. Crystallographic data and refinement details for all four compounds are given in Table 1. Crystallographic data for all structures reported in this paper have been deposited with the Cambridge Crystallographic Data Centre as supplementary publication nos. CCDC-1499906 (**1**), CCDC-1499907 (**2**), CCDC-1499908 (**3**), and CCDC-1499909 (**4**).

Table 1. Crystal data and structure refinement for uranyl compounds **1-4**.

	1	**2**	**3**	**4**
formula	$C_{18.5}H_{14}NO_8U$	$C_{58}H_{48}N_4O_{28}U_4$	$C_{37}H_{28}N_2O_{16}U_2$	$C_{17}H_{11}NO_8U$
formula weight	616.34	2201.13	1232.68	595.30
crystal system	monoclinic	orthorhombic	tetragonal	tetragonal
space group	*C* 2/c	*P* nnm	$P\bar{4}2_1c$	$I\bar{4}2m$
a, Å	14.7897(4)	16.5259(5)	23.5464(3)	24.0601(5)
b, Å	19.8448(5)	16.8232(5)	23.5464(3)	24.0601(5)
c, Å	15.1573(4)	22.9788(7)	20.1023(3)	19.7832(7)
α, deg	90	90	90	90
β, deg	91.940(3)	90	90	90
γ, deg	90	90	90	90
V, Å^3	4446.1(2)	6388.5(3)	11145.4(3)	11452.3(6)
Z	8	4	8	16
T, K	150.01(10)	170(2)	294.82(10)	278(5)
F(000)	1872.0	3588.0	3744.0	3744.0
Dc, g/cm^3	1.841	2.288	1.469	1.381
μ (mm^{-1})	20.785	28.859	16.583	16.139
R_{int}, R_{sigma}	0.0225/0.0323	-/0.0491	0.0350/0.0423	0.0565/0.0557
R_1, wR_2 (I>=2σ (I))	0.0291,0.0710	0.0677,0.1879	0.0308,0.0759	0.0565,0.1618
R_1, wR_2 (all data)	0.0336,0.0730	0.0823,0.1975	0.0390,0.0805	0.0645,0.1700

Computational Methods. Quantum mechanical (QM) calculations were carried out using Gaussian 09 program package[60] with the B3LYP[61-62] hybrid functional. For uranium (U) the quasi-relativistic effective core potentials (RECPs) and the ECP60MWB_SEG basis sets[63-65] were utilized, while the 6-31+G(d) basis sets were used for H, C, O. The simplified model fragments of compounds **1-4** were derived from the X-ray crystal data. Natural population analysis (NPA)[66] and molecular orbital (MO) analysis were performed at the B3LYP/RECP/6-31+G(d) level of theory.

■ RESULTS AND DISCUSSION

Structural Description. *Crystal structure of* ***[UO_2(TP)$_{1.5}$](H_2BPP)$_{0.5}$ (1).*** Compound **1** crystallizes in the *C*2/c space group of monoclinic crystal systme with only one eight-fold coordinated monouranyl center in its asymmetric unit (Figure 2a). The three different **TP** ligand coordinates, together with a uranyl center coordinated by η^2-carboxylic groups, result in a hexagonal bipyramid geometry of uranyl with equatorial U-O distances from 2.436(4) to 2.482(5) Å (Table S1). Moreover, the other ends of the terephthalate ligands connect another three uranyl nodes in different directions (Figure 2b) and extend to form a honeycomb-like 2D network (Figure 2c) with a six-membered ring size of 22.7 Å*17.4 Å (Figure 1). It is interestingly that, unlike the bending topology of the uranyl terephthalate network reported previously[39], all the atoms in the 2D network in compound **1** are nearly coplanar (Figure 2d). Subsequently, based on the regularity of coplanar 2D networks, no parallel interpenetration is aparent. Instead, the honeycomb-like structure of compound **1** achieves closed-packed arrangements directed by strong π-π stacking interactions (Figure 3a-c) as well as by weak hydrogen bonding (Figure S3 and Table S2) between adajcent layers with an interlayer spacing of ~3.3 Å.

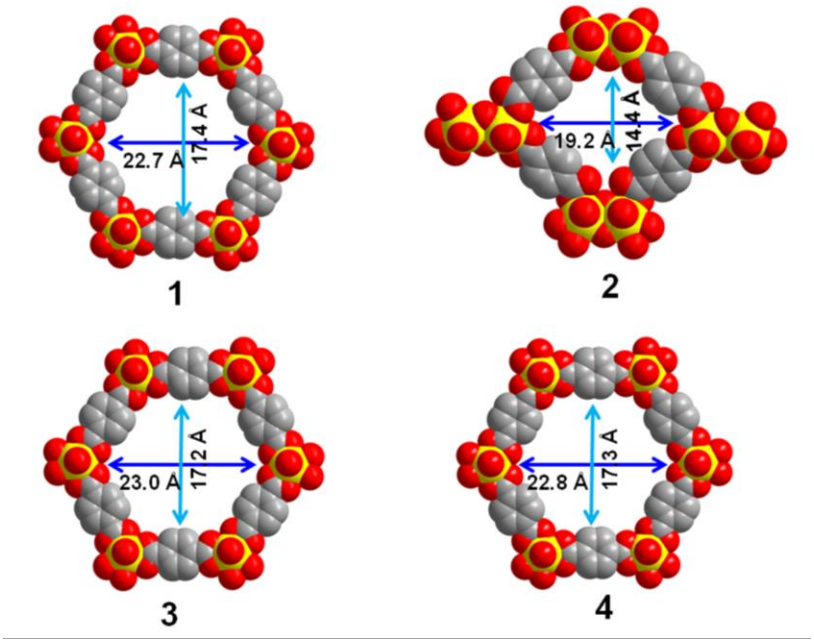

Figure 1. Six-membered or four-membered pores of 2D networks with different ring sizes observed in compounds **1**-**4**. Balls in gray color: carbon atoms; balls in red color: oxygen atoms; balls in yellow color: uranium atoms. All the hydrogen atoms have been omitted for clarity.

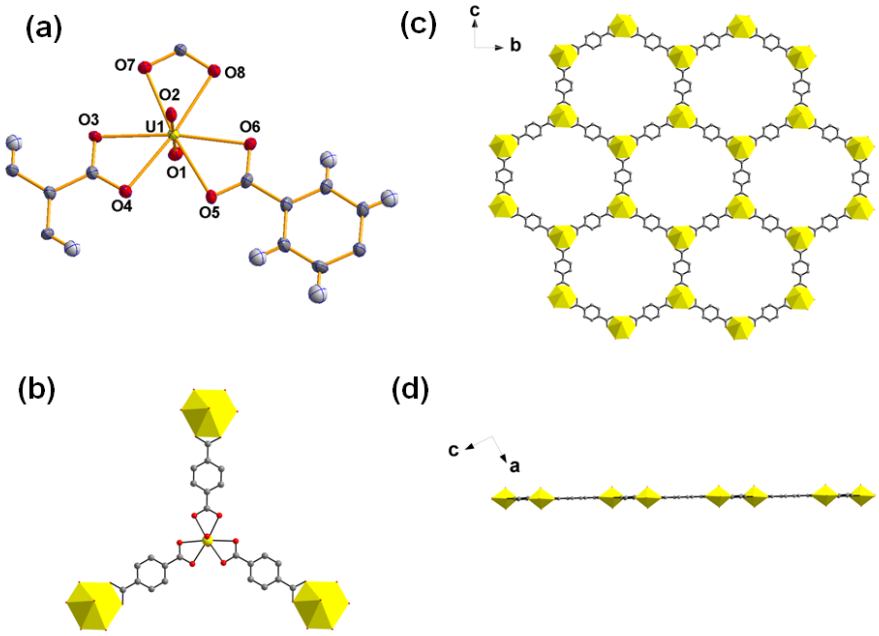

Figure 2. (a) The asymmetric unit of compound **1** containing only one eight-fold coordinated monouranyl center; (b) Coordination sphere of the uranyl center in **1**; (c) The honeycomb-like 2D network viewed from the *a* axis; (d) Lamellar structure of the honeycomb-like 2D network viewed from the *b* axis.

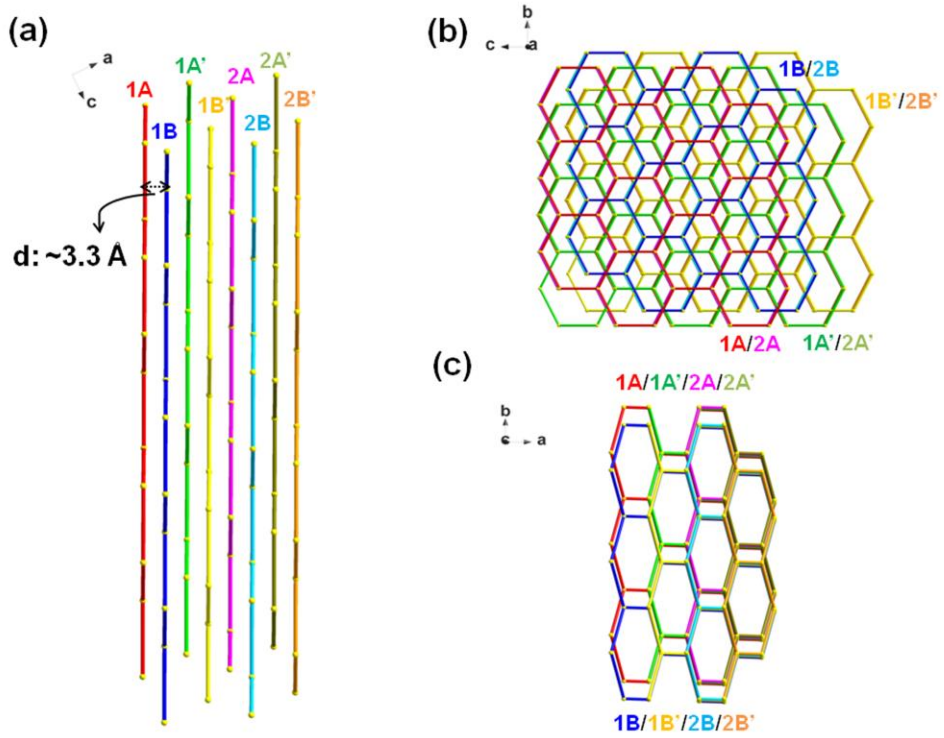

Figure 3. π-π stacking directed closed-packed arrangements of honeycomb-like 2D networks in **1** viewed with an interlayer spacing of 3.3 Å: (a) stacking pattern viewed from the *b* axis bearing eight different layers. (b) stacking pattern viewed from the *a* axis bearing four different layers. (c) stacking pattern viewed from the *c* axis bearing two different layers. Honeycomb-like 2D networks are marked in different colors as a visual aid, and different layers have been labeled with the corresponding name from 1A to 2B'.

Crystal structure of ***[(UO$_2$)$_2$(μ-OH)$_2$(TP)$_2$]$_2$(H$_2$BPP)$_2$ (2).*** The structure of **2**, which crystallizes in the orthorhombic *P*nnm space group, contains two sets of uranyl entities as well as uncoordinated organic base molecules (Figure 4a). A detailed anslysis indicates that both sets of uranyl entities, pointing in two different directions, are dimeric uranyl units (Figure 4b), which give similar coordination spheres and extended structures. Besides being complexed by two bridging OH moieties, each uranyl center in the dimeric unit is also coordinated by another two **TP** ligands in η^2-mode and η^1-mode, respectively, achieving a pentagonal bipyramid geometry of uranyl with equatorial U-O distances from 2.325(13) to 2.486(13) Å for μ(1) and from 2.311(8) to 2.517(12) Å for U(2) (Table S1). These **TP** ligands further connect other uranyl nodes from

different directions, and finally extend to form another rhomboid-shaped 2D network (Figure 4c and 4d). It is notable that all the **TP** linkers connect two adjcent uranyl entries in an asymmetric manner: one end is in η^2-mode, and the other is in η^1-mode, which is unlike the symmetric coordination pattern of the two carboxyl groups of the **TP** linker in **1**.

In terms of stacking in three-dimentional space, two sets of 2D networks aligning along different directions are all polycatenated perpendicularly by each other, which affords the 2D + 2D → 3D reticular polycatenated framework of **2** (Figure 4e). As mentioned above (Scheme 1), uranyl-organic polycatenated frameworks derived from 3,5-di(4-carboxylphenyl) benzoic acid or 4,4'-biphenyldicarboxylic acid represent rare cases of previously reported actinide polycatenated frameworks. The polycatenated framework of **2** found here is another case of this type of entangled structure. Given the larger 2D network ring size (19.2 Å*14.4 Å, see Figure 2) in **2** as compared with the uranyl/3,5-di(4-carboxylphenyl) benzoic acid system (17.2 Å*11.2 Å),[43] it is reasonable that **2** accommodates an inclined polycatenation assembly. It is notable that, unlike the monomeric uranyl node for both previous cases, this is the first uranyl polycatenated framework with oligomeric uranyl SBUs. As shown in Figure 5f, only one rod of one subset passes through each ring of the other inclined subset. All the 2D sheets along the same orientation align in parallel with a spacing distance of 8.6 Å, which results in only one type of cavity with a size of 8.6 Å* 8.6 Å (Figure S4). Similarly to the case of uranyl/4,4'-biphenyldicarboxylate[44], the protonated organic base molecules, **H_2BPP**, are located in the voids formed in the polycatenated framework of **2** and act as the counterions forming the anionic framework (Figure 5). This was confirmed by thermogravimetric analysis of **2**, which shows an distinct peak at 300 °C corresponding to the weight loss of free organic base molecules (Figure S6). Further structural analysis reveals that two types of hydrogen bonds could contribute to the

stability of the polycatenated framework of **2**: one type is hydrogen bonds between adjacent rods in different alignments, and the other is those related with the entrapped **H_2BPP** molecules (Figure S7).

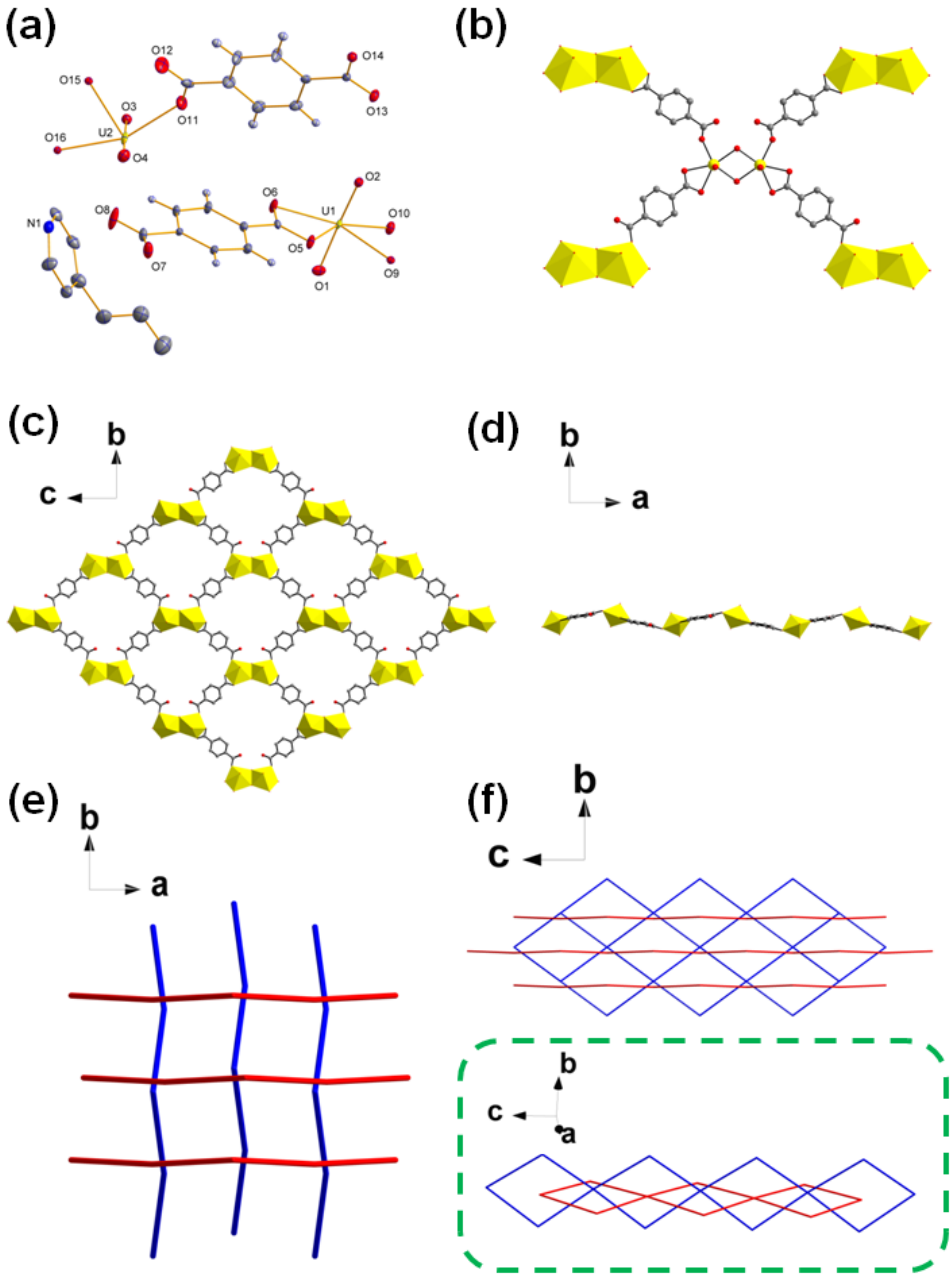

Figure 4. (a) The asymmetric unit of compound **2** containing two similar dimeric uranyl SBUs; (b) coordination sphere of one set of dimeric uranyls in **2**; (c) molecular structures of the 2D rhombus network of **2** viewed from the *a* axis; (d) molecular structures of the 2D rhombus network of of **2** viewed from the *c* axis; (e)

topological diagram of the 2D + 2D → 3D polycatenated framework for **2** viewed from the *c* axis, with the cavity-filling organic base molecules moitted for clarity; (f) topological diagram of the polycatenated framework viewed from the *a* axis and an expanded view with the cavity-filling organic base molecules omitted for clarity. The 2D rhombus networks viewed from two different directions are marked with different colors (blue and red).

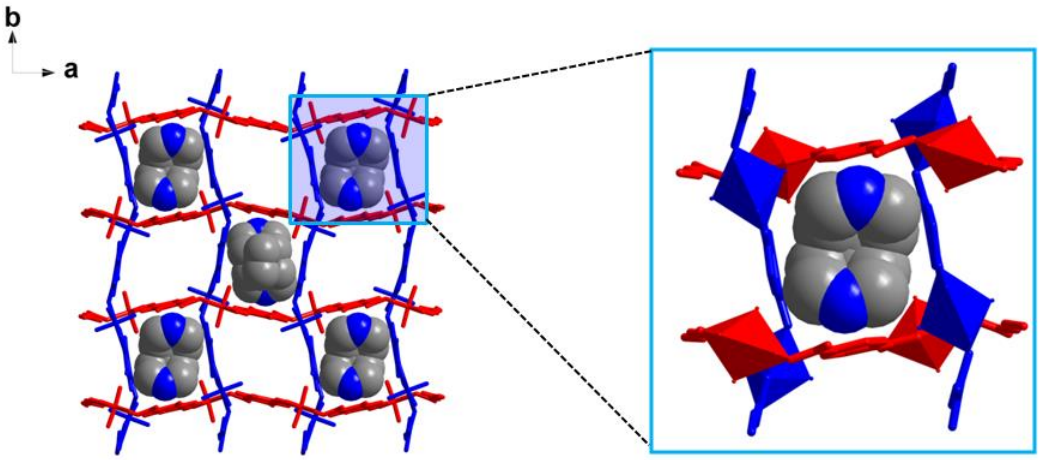

Figure 5. The protonated organic base molecules, **H_2BPP** (shown in the space-filling model), located in the voids formed in the polycatenated framework of **2** (shown in the stick model; the 2D rhombus networks viewed from two different directions are in blue and red, respectively).

Crystal structure of ***[$(UO_2)_2(TP)_3$](H_2BPP) (3).*** The structure of **3**, which crystalizes in the tetragonal $P\bar{4}2_1c$ space group, consists of two different uranyl centers (U(1) and U(2)) as well as three **TP** ligands in its asymmetric unit (Figure 6a). Both of the uranyl centers are coordinated with three η^2-carboxylate groups of **TP** ligands, resulting in a hexagonal bipyramid geometry (Figure 6b). Similar to compound **1**, the uranyl nodes are connected by **TP** ligands to achieve a honeycomb-like 2D network. However, due to the non-equivalence of U(1) and U(2) in **3**, its coplanarity is reduced in comparison with **1**, resuting in a bending topology when viewed from the *c* axis (Figure 6c and 6d). Furthermore, in terms of crystal stacking in three-dimentional space, a 2D + 2D → 3D reticular polycatenated framework occurs again for compound **3** (Figure 6e and 6f). Detailed analysis shows that there are two grids having two rings of one set

passing through each ring from the other inclined subset. Each ring of one grid passes through two adjacent grids, which indicates a higher degree of catenation than in **2**. Interestingly, each set of two bent grids in one ring align in parallel with a spacing distance of 7.6 Å, while those adjacent bent grids in different rings align in an anti-parallel mode with a maximum distance of 9.0 Å and a minimum distance of 7.9 Å (Figure S4). This distinctive assembly affords three types of irregular cavities with different sizes. Considering the different ring sizes of 2D networks in **2** and **3**, the higher degree of catenation for **3** may be attributed to the larger size of the six-membered honeycomb-like ring, 23.0 Å*17.2 Å (Figure 1). Hydrogen bonding networks between adjacent rods in different alignments were also found, which should contribute to the cross-linking of the polycatenated framework in **3** (Figure S8 and Table S2).

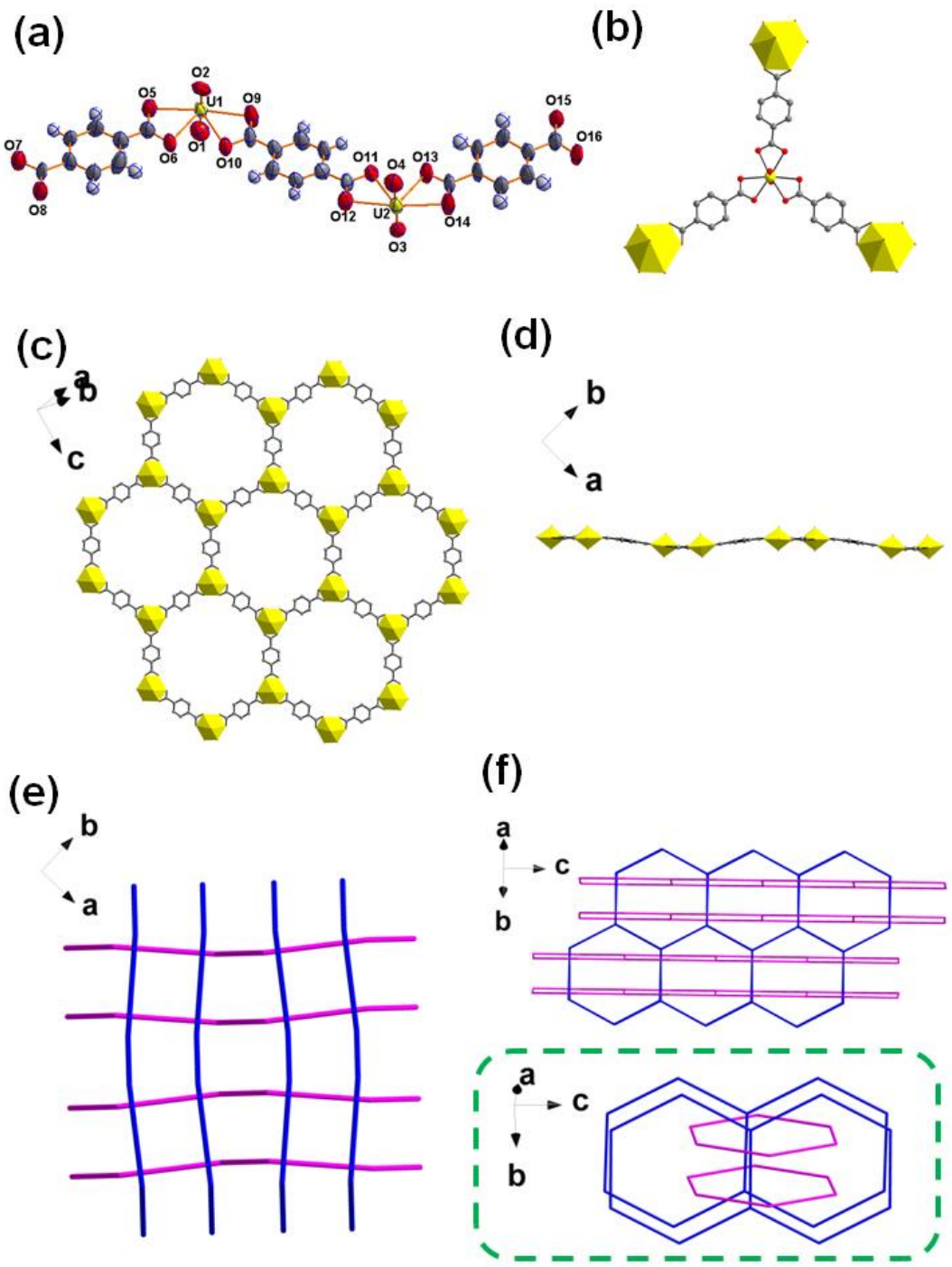

Figure 6. (a) The asymmetric unit of compound **3** containing two different uranyl centers U(1) and U(2); (b) coordination sphere of one uranyl (U1) in **3**; (c) molecular structures of the honeycomb-like 2D network viewed along the (1, 1, 0) face; (d) molecular structures of honeycomb-like 2D network viewed from the *c* axis; (e) topological diagram of 2D + 2D → 3D polycatenated frameworks for compound **3** viewed from the *c* axis; (f) topological diagram of part of polycatenated framework viewed along the (1, 1, 0) face, an expanded view.

The 2D rhombus networks viewed from two different directions are marked with different colors (blue and pink).

Crystal structure of ***$[UO_2(TP)_{1.5}](H_2BPY)_{0.5}$*** *(4).* Compound **4** was synthesized by a hydrothermal reaction procedure similar to that used for compound **1,** except that more rigid but smaller **BPY** replace **BPP** molecules. Compound **4** crystallizes in the tetragonal $I\bar{4}2m$ space group. Interestingly, despite the different crystal system and space group for compounds **1** and **4**, the asymmetric unit of **4** is idential to that of **1** (Figure 7a). Accordingly, the coordination sphere of uranyl and extended honeycomb-like 2D network of **4** are also similar to those of **1** (Figure 7b-d). The consistency of the basic structural unit for **1** and **4** suggests very similar crystal structures, which is consistent with the similar synthesis protocols for **1** and **4**. The most striking distinction between **4** and **1** is their crystal packing structures; compound **4** achieves its lattice packing through an inclined polycatenation mode (Figure 7e-7f). As shown in Figure 8f, two sets of grids pass perpendicularly through each ring of the other inclined subset in the polycatenated framework of **4.** Similar to **3**, each set of two flat layered grids in one ring align in parallel with a spacing distance of 7.9 Å, while adjacent flat layered grids in different rings align in parallel with a spacing distance of 9.1 Å (Figure S4). Similar to **3**, hydrogen bonding networks between adjacent rods in different alignments were also found in **4** (Figure S8 and Table S2), which should contribute to the cross-linking of the polycatenated framework. This type of assembly affords three kinds of regular cavities of different sizes (7.9 Å * 7.9 Å, 7.9 Å * 9.1 Å and 9.1 Å * 9.1 Å, Figure S4). The catenation mode here can be attributed to the modest size of the six-membered ring of the 2D networks in **4** (Figure 1), just as for **3** with similar honeycomb-like rings in bent 2D sheets.

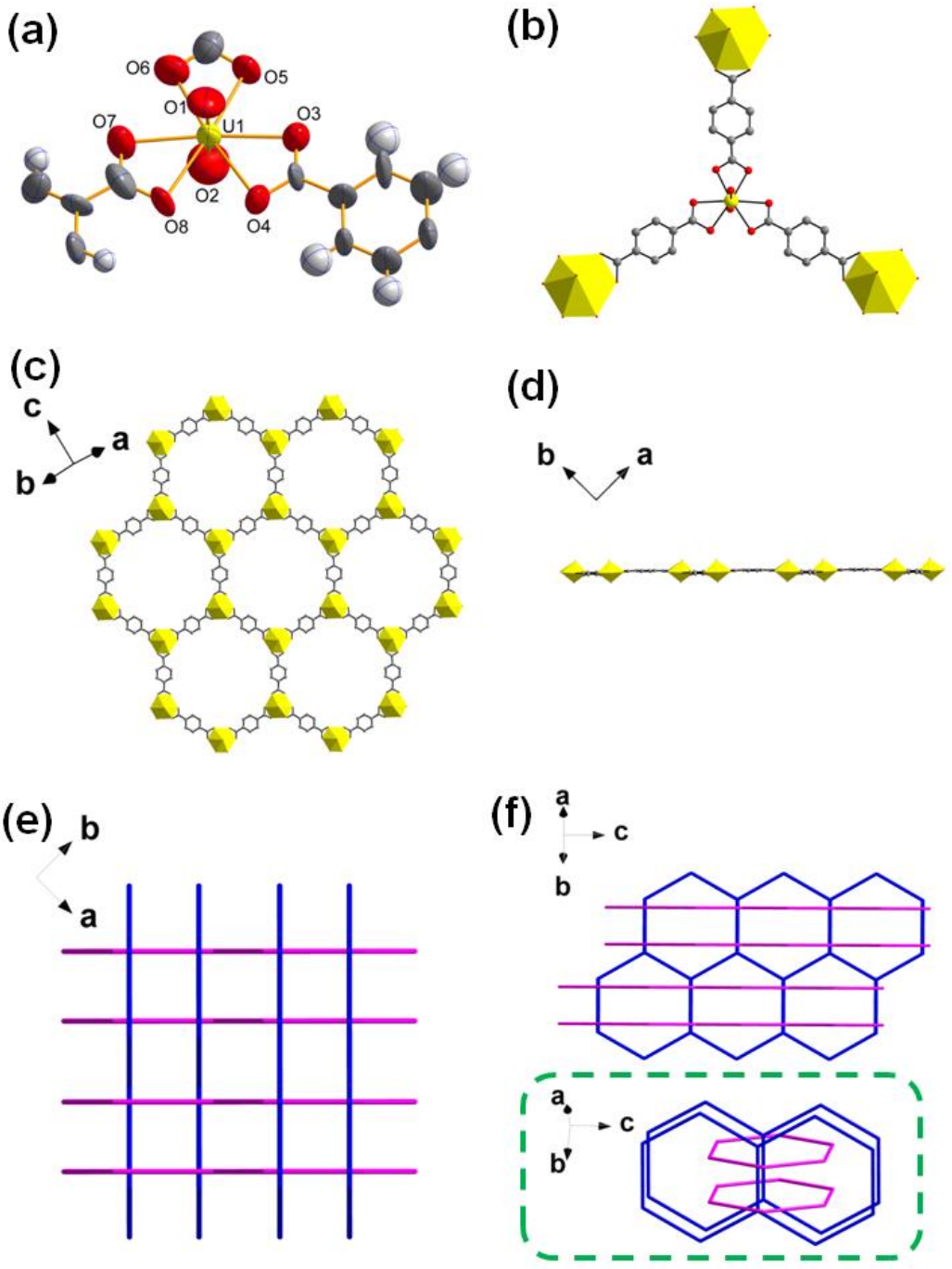

Figure 7. (a) The asymmetric unit of compound **4** wtih a monouranyl center; (b) coordination sphere of uranyl in **4**; (c) molecular structures of honeycomb-like 2D network viewed along the (1, 1, 0) plane; (d) molecular structures of honeycomb-like 2D network viewed from the *c* axis; (e) topological diagram of the 2D + 2D → 3D polycatenated frameworks for compound **4** viewed from the *c* axis; (f) topological diagram of part of the polycatenated framework and its close view. The 2D rhombus networks viewed from two different directions are marked with different colors (blue and pink).

pH-dependent structural regulation of uranyl terephthalate compounds. Compounds **1-4** were synthesized from a mixture of uranyl nitrate hexahydrate and H_2**TP** ligand in the presence of **BPP** or **BPY** in aqueous medium at different pH values. The initial hydrothermal syntheses from uranyl nitrate hexahydrate, H_2**TP** and **BPP** without any NaOH added produced unkonwn light yellow plate-like microcrystal products (Figure S9a), which could not be identified by single-crystal or powder X-ray diffraction. Addition of a small amount of sodium hydroxide (NaOH/$\mathbf{H_2TP}$ = 0.5-1.0) to the mixture of uranyl and terephthalic acid leads to the formation of **1** with non-interpenetration the honeycomb-like structure (Figure S9b with NaOH/$\mathbf{H_2TP}$ = 0.5, final aqueous pH of 4.28), which is similar to the previously-reported uranyl-**TP** systems.[39, 52] It is reasonable that the addition of NaOH promotes the deprotonation of terephthalic acid ($\mathbf{H_2TP}$), thus facilitating the coordination of uranyl by terephthalate (**TP**) group. When the amount of NaOH is increased up to over 1 equivalent ($\mathbf{OH^-/H_2TP}$ = 1.0-2.0), which means an elevation of the solution pH as well as more deprotonation of terephthalic acid (the final pH of the aqueous solution is increased to 5.21-7.00), can promote the formation of a dimeric uranyl-mediated polycatenated framework (**2)** (Figure S9c with NaOH/$\mathbf{H_2TP}$ = 1.5 at a final aqueous pH of 6.11). As the pH of the aqueous solution under hydrothermal conditions was increased gradually, a new phase of monomeric uranyl-mediated polycatenated framework (**3**) begins to emerge. Detailed PXRD analysis (Figure 8) demonstrates that the crystal phase of **3** does not appear until the pH is increased to 6.61 ($\mathbf{OH^-/H_2TP}$ = 1.75), and becomes significant product at a pH of 7.00 (Figure S9d with with NaOH/$\mathbf{H_2TP}$ = 2.0). Regarding the special role of **BPP**, this pH-regulated process might be related to different behavior of **BPP** at varying pH, which exerts an indirect influence on uranyl coordination and lattice packing. Similar regulation of supramolecular isomers has been observed in a 2, 9-phenanthroline-based uranyl-organic hydrothermal system reported by

our group.[17] Interestingly, when using more rigid but small-size **BPY** replace **BPP** molecules, the polycatenated framework of compound **4** was obtained from a relatively acidic solution (NaOH/$\mathbf{H_2TP}$ = 0.5, similar to that of compound **1**). The remarkable structural difference between **4** and **1**, which synthesized respectively from **BPY** and **BPP** under nearly identical aqueous condition, suggests different behaviors of **BPY** and **BPP** in mediating the assembly of uranyl-terephthalate coordination systems. Overall, the preparation of compounds **1**-**4** displays an interesting pH-dependent evolution, which could be tuned by adjusting the acidity of aqueous solutions (Figure 9). In particular, the similarity of basic building units for **1**, **3** and **4**, which could be taken as different polymorphs when neglecting the counter-ions, suggests a crucial effect of pH on polymorph formation.

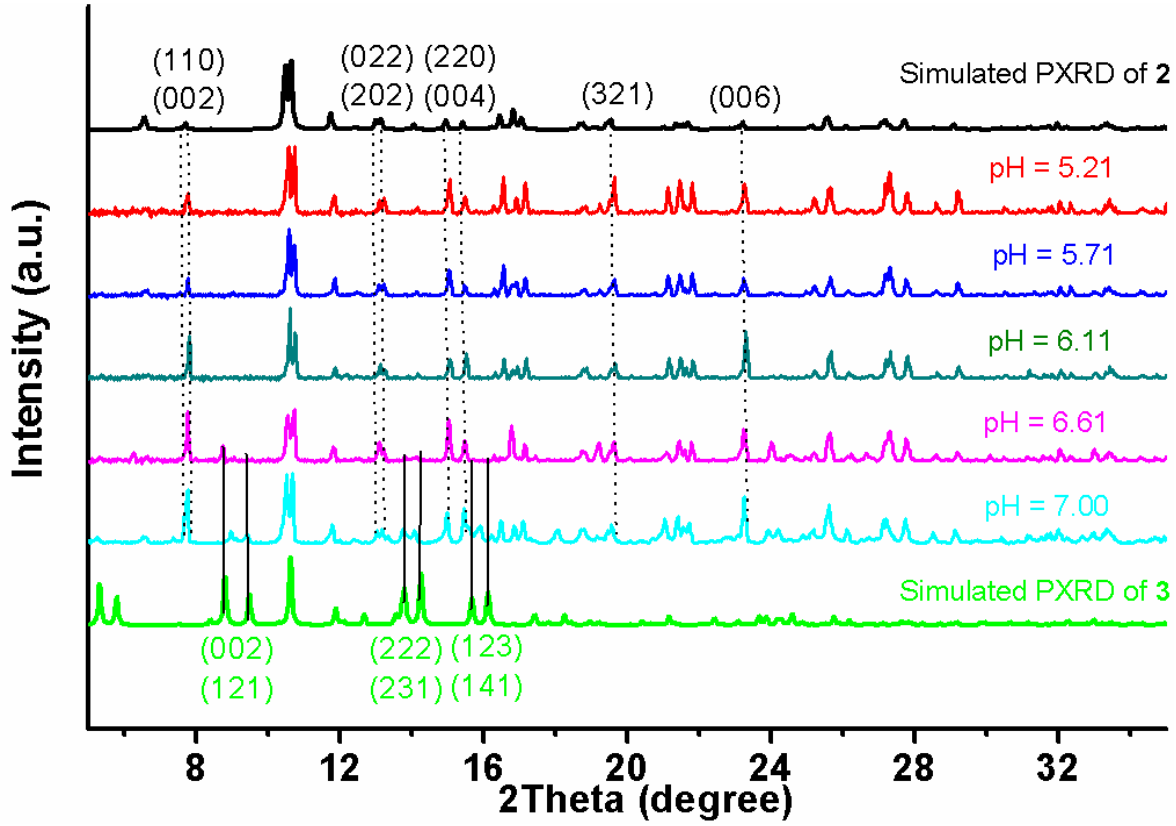

Figure 8. PXRD patterns demonstrating the evolution of crystal phase from pure compound **2** to a mixture of **2** and **3** along with the gradual increase of pH values in the hydrothermal system of uranyl-**H_2TP-BPP**. Numbers in brackets correspond to the diffraction indices of diffraction peaks.

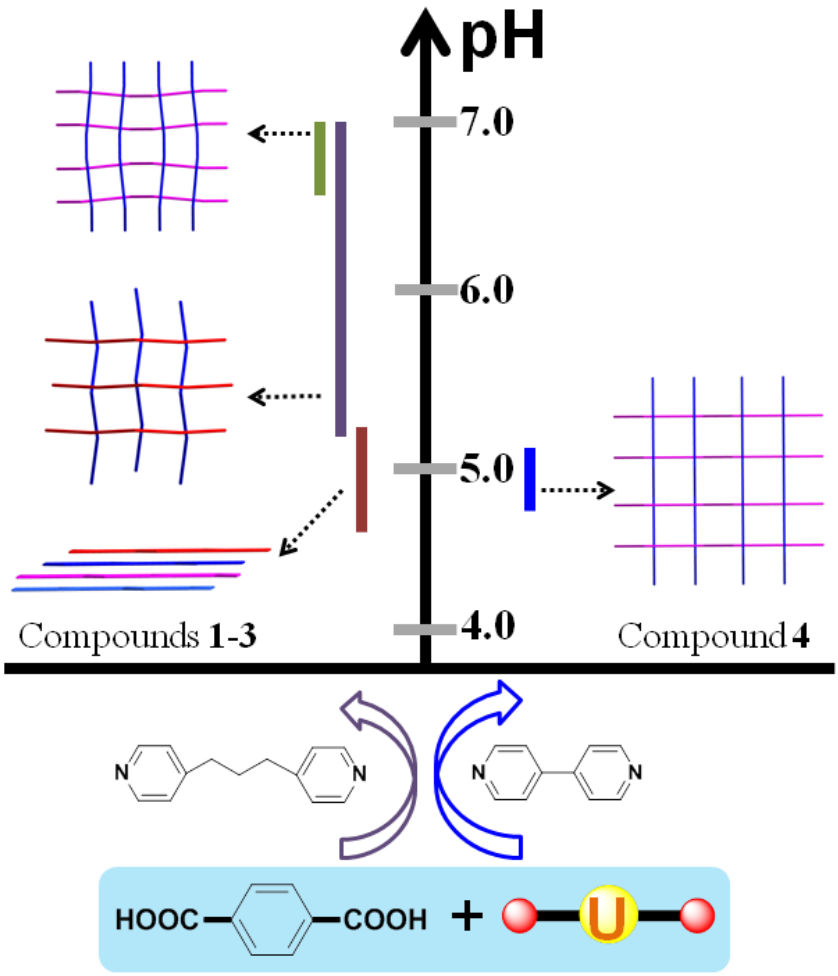

Figure 9. pH-dependent structural regulation of uranyl terephthalate compounds **1-4**.

The role of BPP or BPY organic base on the formation of uranyl terephthalate polycatenated frameworks. As a very simple aromatic acid, terephthalic acid (**H_2TP**) has attracted continuous research interests from inorganic chemists specialized in actinide-organic hybrid materials. Following the early work on uranyl terephthalate coordination polymers by Chen et al[48] and Jacobson et al[39], extensive exploration of new uranyl terephthalate compounds

using an additional organic base (terpyridines,[50, 53] 2,4,6-tris(2-pyridyl) striazine,[17, 49] 2,2′-bipyridine[37] or 1-(4-(1H-imidazol-1-yl)-2,5-dimethylphenyl)-1H-imidazole[38]) have been conducted. Although several non-interpenetrating or interpenetrating uranyl terephthalate networks and frameworks have been prepared (Figure S10), no uranyl terephthalate compounds with 2D→3D polycatenated frameworks have been identified in these systems. In this work, the strategy of introducing **BPP** or **BPY** organic base molecules into the reaction system of uranyl-terephthalic acid successfully promotes the formation of polycatenated frameworks under hydrothermal conditions. This inclined polycatenation assembly results in a higher degree of assembly and higher symmetry as indicated by the crystal systems and space groups of compounds **2**-**4**. Similar phenomena can be found for the other uranyl compounds with polycatenated frameworks, [42-44] which also yield high-symmetry space groups.

In order to evaluate the role of **BPP** or **BPY** organic base in the formation of uranyl terephthalate polycatenated frameworks, a set of control experiments were performed under similar conditions except the for utilization of **BPP** or **BPY** (see EXPERIMENTAL SECTION). The experimental results showed formation of only transparent stick crystals of H_2**TP** at lower pH (Figure S11a-e), or at higher pH light yellow microcrystal that could not be characterized (Figure S11f-h and Figure S12). The clear distinction between the reactions without **BPP** or **BPY** and those in the presence of **BPP** or **BPY** reveals the important role of the organic base for the synthesis of well-crystallized uranyl terephthalate compounds with polycatenated frameworks. We also conducted a direct comparison between the uranyl terephthalate system with **BPP** or **BPY** reported here with previoulsy reported systems utilizing other organic bases such as 2,2′-bipyridine[37] or 1-(4-(1H-imidazol-1-yl)-2,5-dimethylphenyl)-1H-imidazole.[38] It is interesting to find that, although there are some similarities in molecular structures for these

different organic bases, the coordination behaviors are very different. Unlike 2,2′-bipyridine or 1-(4-(1H-imidazol-1-yl)-2,5-dimethylphenyl)-1H-imidazole as auxiliary ligands in the coordination sphere of the uranyl center, for **BPP** or **BPY** this is not the case, which might be related to its mismatching with terephthalate ligand in molecular size.[67] This difference indicates that non-coordinated organic bases seem to be more suitable to construct polycatenated frameworks by serving as the template and cavity-filling agent, while the organic base molecules coordinated to uranyl alter the coordination pattern of metal center, as well as lack cavity-filling agents. Similar templated syntheses have been observed in other previously reported uranyl-organic polycatenated frameworks based on 4,4′-biphenyldicarboxylate[44] or 2,5-thiophenedicarboxylate ligands,[45] where $[Ni(bipy)_3]^{2+}$ or $[Ag(bipy)_2]^{+}$ counter ions are the bulking template agent for the polycatenated frameworks. It should be noted that our discussion here is specific to the uranyl terephthalate system or similar uranyl coordination polymers with rigid aromatic carboxylate ligand system. There are exceptions for other organic ligand systems, such as a polycatenated framework found in a uranyl compound with mixed ligands of flexible adipic acid and 4,4′-bipyridine.[42]

Besides non-coordinated **BPP** or **BPY** organic base molecules, other specific factors, especially reaction conditions, are also important for the construction of uranyl terephthalate polycatenated frameworks. For example, relatively acidic conditions only promote the formation of compound **1** with a 2D network structure, not a polycatenated framework, even in the presence of **BPP**. Similarly, a recently reported uranyl terephthalate compound with non-coordinated 2,4,6-tris(2-pyridyl) striazine organic base did not form a polycatenated framework due to a lack of 2D networks as basic building blocks.[49] Therefore, it can be concluded that the template and cavity-filling effect of organic bases (such as **BPP** or **BPY**) in combination with the

specific hydrothermal conditions promote the formaion of uranyl terephthalate polycatenated frameworks.

Fluorescence properties. The fluorescence of the uranyl cation features five or six vibronic peaks in the range of 450 to 650 nm, which arise from electronic transitions between the LUMO 5f non-bonding uranyl orbitals and the HOMO U−O hybrid sigma bonding orbital, referred to as U=O axial ligand-to-metal charge transfer (LMCT) bands.[68] Fluorescence spectra under excitation at a wavelength of 420 nm were recorded for compounds **1** and **2** (pure **3** and **4** could not be isolated in sufficient yields). As shown in Figure 10, compound **1** displays quenching of uranyl luminescence. Considering the close-packing in the layered structure of **1**, the lack of emission is likely due to the spatial proximity of adjacent 2D layers, which may result in non-radiative decay of uranyl luminescence.[69] The geometric structure of uranyl, as well as uranyl species, affects the fluorescence features and specific positions of emission peaks. [44, 70-71] Unlike compound **1** in a hexagonal bipyramidal coordination geometry, the emission spectrum of compound **2** with a pentagonal bipyramidal geometry gives the typical vibronic progression of uranium (VI) with the five main emission bands located at 501 (s), 521 (s), 544 (m), 569 (m) and 596 (w) nm corresponding to the $S_{11} \rightarrow S_{00}$ and $S_{10} \rightarrow S_{0v}$ ($v = 0-4$) electronic transitions.[72] These bands are red-shifted relative to that of other fluorescent uranyl-organic compounds with similar uranyl dimer units showing pentagonal pyramids sharing a common edge (e.g. $UO_2(C_5H_6O_4)$[73-74] and $UO_2(C_6H_8O_4)$[74-75]). This emission peak red-shift may be attributed to the different seven-fold coordination environment the uranyl center in these compounds. The most significant difference in the coordination environments are the bridging groups between the uranyl-centered polyhedra, which in compound **2** are hydroxo bridges (-OH), whereas in $UO_2(C_5H_6O_4)$ or $UO_2(C_6H_8O_4)$ they are μ_3-O atoms from ligand carboxyl groups (Figure S13).

Besides the bridging groups, there are differences in number and coordination pattern of carboxyl groups coordinated to the uranyl centers (one monodentate carboxyl and one bidentate carboxyl for compound **2**; two monodentate carboxyls and half a bidentate carboxyl for $UO_2(C_6H_8O_4)$), as well as the type of spacers (phenyl linker for compound **2**; C4 linker for $UO_2(C_6H_8O_4)$) (Figure S13). These latter structural differences likely also affect fluorescence properties of the uranyl coordination compounds.

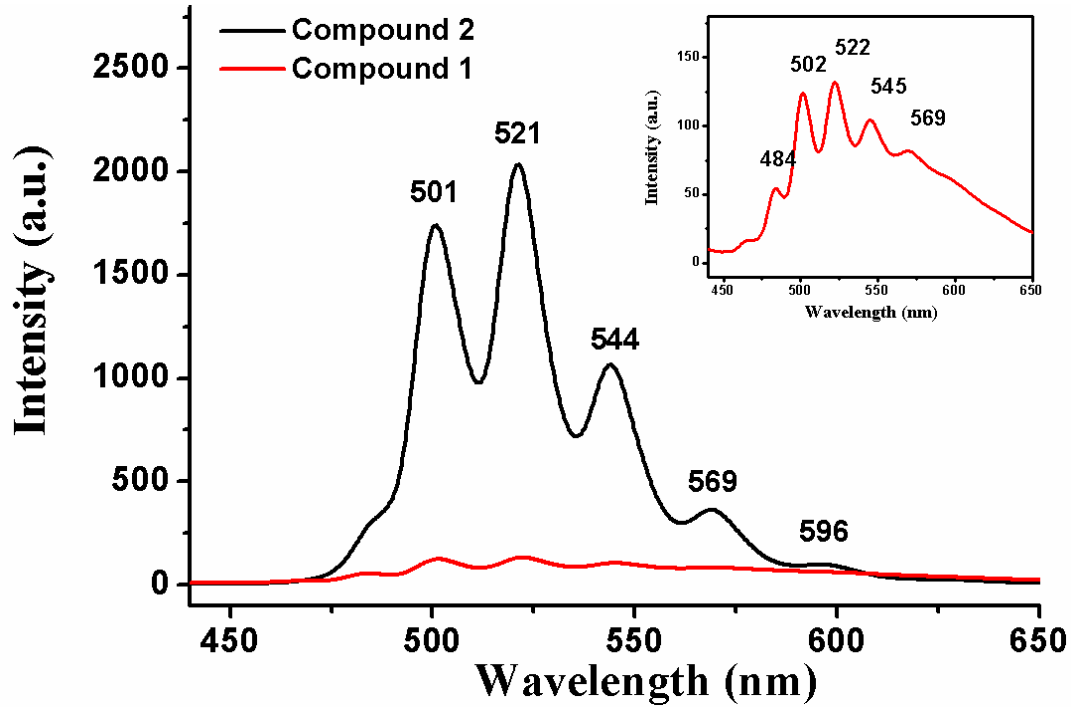

Figure 10. The fluorescence spectra of compounds **1** and **2** with excitation wavelength at 420 nm (insert: enlarged fluorescence spectrum of **1**).

Quantum mechanical (QM) calculations. As demonstrated above, the molecular structures of compounds **1**-**4** are all based on a uranyl-terephthalate backbone but display different bonding features and topologies. In particular, compounds **1**, **3** and **4**, which could be taken as different polymorphs if not for the counter-ions, show nearly identical basic building units. To explore the nature of the metal-ligand bonding in compounds **1**-**4**, theoretical analysis via QM calculations[61-

[62] was conducted. To simplify this analysis, electronic structures of the model fragments of these compounds (Figure 11) were studied using density functional theory (DFT) method. For all the model fragments, the predicted uranium atomic charge are found to be in the range 1.38-1.54, which is much lower than in the free UO_2^{2+} cation (2.81), indicating substantial charge transfer from the ligands to the uranyl centers. According to molecular orbital analysis for all the compounds (Figures 12, and S14-S16), the lowest unoccupied molecular orbitals (LUMOs) are mainly concentrated on the 5f orbitals of uranium, while the highest occupied molecular orbitals (HOMOs) are mainly located in the ligand benzene rings. The metal-ligand σ-bonding orbitals apparent in all these compounds mainly result from the U 5f, 6d, 7s and O 2p orbital interactions.

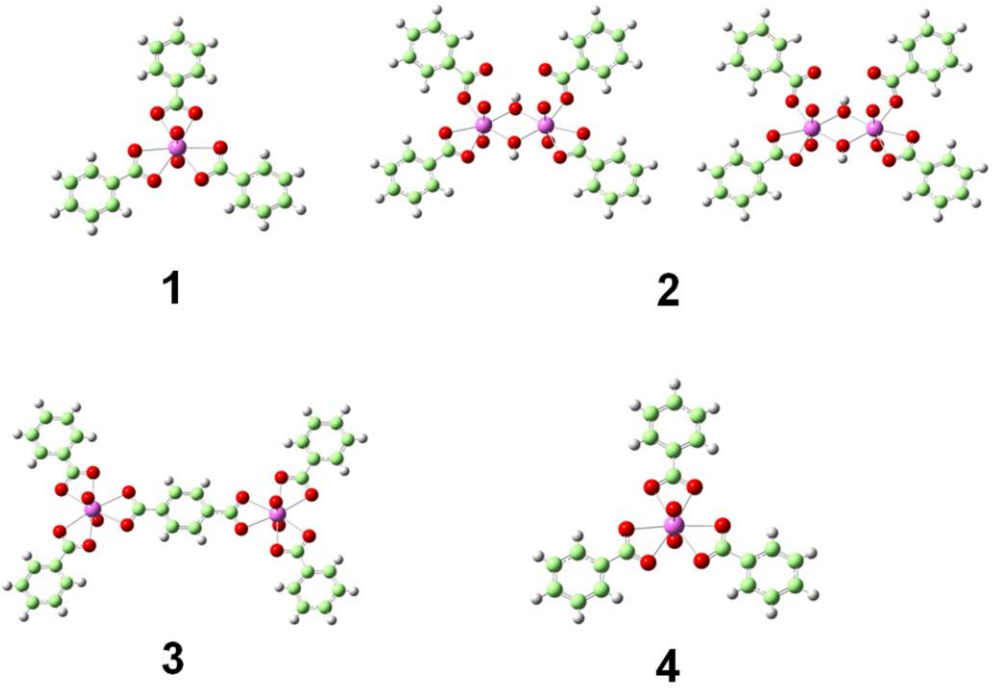

Figure 11. Simplified model fragments of compounds **1-4** tailored from the minimum structural units. Green, red, and pink spheres represent C, O, N, and U, respectively.

Figure 12. The LUMO (a, j), HOMO (b, k) orbitals and the main MOs (c-i, l-r) of the U-O bonding for the model fragments of compound **2**.

For compound **1** (Figure S14), the U-O σ-bonding orbital (1c orbital) contain 8% uranium 5f orbital character and 14% oxygen 2p orbital character. The 1d orbital of the U-O σ-bonding is composed of 12% U 7s character and 8% O 2p character. Similar to compound **1**, the 4c and 4d, 4e orbitals of compound **4** (Figure S16) correspond to the U-O σ-bonding orbitals. The former orbitals come from U 5f and O 2p orbital interactions, while the latter orbitals result from the interactions of U 5f, 6d, 7s and O 2p orbitals. For the two model fragments of compound **2** (Figure 12), similar MOs are found due to similar structural parameters of these fragments. The 2c, 2d, 2l, 2m and 2n orbitals correspond to the σ-bonding orbitals between the uranyl and the oxygen atoms of the carboxyl ligands, which show

some differences in the magnitude of the orbital compositions (2c and 2d: U 5f and 6d orbitals; 2l, 2m and 2n: U 5f or 6d orbital). Other orbitals correspond to the σ-bonding orbitals between the uranyl and the oxygen atoms of the bridging hydroxyl groups mainly resulting from the U 5f, 6d, 7s and O 2p orbital interactions. For compound **3** (Figure S15), the 3c and 3d orbitals are the U-O σ-bonding orbitals originating from the interactions of U 6d, 7s orbitals and O 2p orbitals, while the 3e, 3f, 3g and 3h orbitals represent the U-O σ-bonding orbitals resulted from U 5f and O 2p orbital interactions. In all, the DFT calculations provide insights about uranium-ligand bonding features in compounds **1**-**4**.

■ CONCLUSIONS

In this work, we present the assembly of uranyl-organic polycatenated frameworks from terephthalic acid through a templated-synthsis method using organic bases **BPP** or **BPY** for the first time. A pH-dependent structural variation has been found, which results in a series of novel uranyl-terephthalate polycatenated frameworks **2**-**4**. DFT calculations afford detailed information on the uranium-ligand bonding features of all the four compounds **1**-**4**. A direct comparison between these polycatenated frameworks and previously-reported uranyl terephthalate compounds suggests that the template and cavity-filling effect of organic bases (such as **BPP** or **BPY**) in combination with the specific hydrothermal conditions promote the formaion of uranyl terephthalate polycatenated frameworks. The intriguing polycatenated frameworks found here enriches the family of actinide polycatenated frameworks, and also provides another interesting case of pH-dependent structural regulation for uranyl compounds.

■ ASSOCIATED CONTENT

Supporting Information

Typical figures including powder X-ray diffraction and thermogravimetric analysis, typical crystal and topological structures, calculation results of compounds **1** and **4** are included. This material is available free of charge via the Internet at http://pubs.acs.org.

■ AUTHOR INFORMATION

Corresponding Authors

*E-mail: shiwq@ihep.ac.cn.

Notes

The authors declare no competing financial interests.

■ ACKNOWLEDGMENT

We thank the support of this work by the National Natural Science Foundation of China (21671191, 21577144 and 11405186) and the Major Resarch Plan "Breeding and Transmutation of Nuclear Fuel in Advanced Nuclear Fission Energy System" of the Natural Science Foundation of China (91426302 and 91326202) and the Science Challenge Project (JCKY2016212A504). We appreciate the help from Prof. Daofeng Sun and Dr. Liangliang Zhang for X-ray single crystal measurements.

■ REFERENCES

[1] Jones, M. B.; Gaunt, A. J., Recent Developments in Synthesis and Structural Chemistry of Nonaqueous Actinide Complexes. *Chem. Rev.* **2013,** *113*, 1137-1198.

[2] Dam, H. H.; Reinhoudt, D. N.; Verboom, W., Multicoordinate Ligands for Actinide/Lanthanide Separations. *Chem. Soc. Rev.* **2007,** *36*, 367-377.

[3] Szabo, Z.; Toraishi, T.; Vallet, V.; Grenthe, I., Solution Coordination Chemistry of Actinides: Thermodynamics, Structure and Reaction Mechanisms. *Coord. Chem. Rev.* **2006,** *250*, 784-815.

[4] Moore, K. T.; van der Laan, G., Nature of the 5f States in Actinide Metals. *Rev. Mod. Phys.* **2009,** *81*, 235-298.

[5] Burns, P. C.; Ewing, R. C.; Hawthorne, F. C., The crystal chemistry of hexavalent uranium: Polyhedron geometries, bond-valence parameters, and polymerization of polyhedra. *Can Mineral* **1997,** *35*, 1551-1570.

[6] Dembowski, M.; Olds, T. A.; Pellegrini, K. L.; Hoffmann, C.; Wang, X. P.; Hickam, S.; He, J. H.; Oliver, A. G.; Burns, P. C., Solution ^{31}P NMR Study of the Acid-Catalyzed Formation of a Highly Charged $\{U_{24}Pp_{12}\}$ Nanocluster, $[(UO_2)_{24}(O_2)_{24}(P_2O_7)_{12}]^{48-}$, and Its Structural Characterization in the Solid State Using Single-Crystal Neutron Diffraction. *J. Am. Chem. Soc.* **2016,** *138*, 8547-8553.

[7] Acher, E.; Cherkaski, Y. H.; Dumas, T.; Tamain, C.; Guillaumont, D.; Boubals, N.; Javierre, G.; Hennig, C.; Solar, P. L.; Charbonnel, M. C., Structures of Plutonium(IV) and Uranium(VI) with N,N-Dialkyl Amides from Crystallography, X-ray Absorption Spectra, and Theoretical Calculations. *Inorg. Chem.* **2016,** *55*, 5558-5569.

[8] Knope, K. E.; Soderholm, L., Solution and Solid-State Structural Chemistry of Actinide Hydrates and Their Hydrolysis and Condensation Products. *Chem. Rev.* **2013,** *113*, 944-994.

[9] Wang, K. X.; Chen, J. S., Extended Structures and Physicochemical Properties of Uranyl-Organic Compounds. *Acc. Chem. Res.* **2011,** *44*, 531-540.

[10] Loiseau, T.; Mihalcea, I.; Henry, N.; Volkringer, C., The Crystal Chemistry of Uranium Carboxylates. *Coord. Chem. Rev.* **2014,** *266*, 69-109.

[11] Andrews, M. B.; Cahill, C. L., Uranyl Bearing Hybrid Materials: Synthesis, Speciation, and Solid-State Structures. *Chem. Rev.* **2013,** *113*, 1121-1136.

[12] Falaise, C.; Volkringer, C.; Vigier, J. F.; Henry, N.; Beaurain, A.; Loiseau, T., Three-Dimensional MOF-Type Architectures with Tetravalent Uranium Hexanuclear Motifs (U6O8). *Chem. Eur. J.* **2013,** *19*, 5324-5331.

[13] Falaise, C.; Assen, A.; Mihalcea, I.; Volkringer, C.; Mesbah, A.; Dacheux, N.; Loiseau, T., Coordination polymers of uranium(IV) terephthalates. *Dalton Trans.* **2015,** *44*, 2639-2649.

[14] Falaise, C.; Volkringer, C.; Loiseau, T., Mixed Formate-Dicarboxylate Coordination Polymers with Tetravalent Uranium: Occurrence of Tetranuclear {U4O4} and Hexanuclear {U6O4(OH)(4)} Motifs. *Cryst. Growth Des.* **2013,** *13*, 3225-3231.

[15] Mei, L.; Wu, Q. Y.; Liu, C. M.; Zhao, Y. L.; Chai, Z. F.; Shi, W. Q., The first case of an actinide polyrotaxane incorporating cucurbituril: a unique 'dragon-like' twist induced by a specific coordination pattern of uranium. *Chemical Communications* **2014,** *50*, 3612-3615.

[16] Zhu, L. Z.; Wang, C. Z.; Mei, L.; Wang, L.; Liu, Y. H.; Zhu, Z. T.; Zhao, Y. L.; Chai, Z. F.; Shi, W. Q., Two Novel Uranyl Complexes of Semi-rigid Aromatic Tetracarboxylic Acid Supported by Organic Base as Auxiliary Ligand or Templating Agent: an Experimental and Theoretical Exploration. *Crystengcomm* **2015,** *17*, 3031-3040.

[17] An, S. W.; Mei, L.; Wang, C. Z.; Xia, C. Q.; Chai, Z. F.; Shi, W. Q., The first case of actinide triple helices: pH-dependent structural evolution and kinetically-controlled transformation of two supramolecular conformational isomers. *Chemical Communications* **2015,** *51*, 8978-8981.
[18] Mei, L.; Wang, L.; Yuan, L. Y.; An, S. W.; Zhao, Y. L.; Chai, Z. F.; Burns, P. C.; Shi, W. Q., Supramolecular Inclusion-Based Molecular Integral Rigidity: A Feasible Strategy for Controlling Structural Connectivity of Uranyl Polyrotaxane Networks. *Chem. Commun.* **2015,** *51*, 11990-11993.
[19] An, S. W.; Mei, L.; Hu, K. Q.; Xia, C. Q.; Chai, Z. F.; Shi, W. Q., The templated synthesis of a unique type of tetra-nuclear uranyl-mediated two-fold interpenetrating uranyl-organic framework. *Chem. Commun.* **2016,** *52*, 1641-1644.
[20] Thuery, P., Uranyl Ion Complexes with Cucurbit[n]urils (n=6, 7, and 8): A New Family of Uranyl-Organic Frameworks. *Cryst. Growth Des.* **2008,** *8*, 4132-4143.
[21] Liao, Z. L.; Li, G. D.; Bi, M. H.; Chen, J. S., Preparation, Structures and Photocatalytic Properties of Three New Uranyl-organic Assembly Compounds. *Inorg. Chem.* **2008,** *47*, 4844-4853.
[22] Wang, H.; Chang, Z.; Li, Y.; Wen, R. M.; Bu, X. H., Chiral Uranyl-Organic Compounds Assembled with Achiral Furandicarboxylic Acid by Spontaneous Resolution. *Chem. Commun.* **2013,** *49*, 6659-6661.
[23] Mihalcea, I.; Henry, N.; Bousquet, T.; Volkringer, C.; Loiseau, T., Six-Fold Coordinated Uranyl Cations in Extended Coordination Polymers. *Crystal Growth & Design* **2012,** *12*, 4641-4648.
[24] Mei, L.; Wu, Q. Y.; An, S. W.; Gao, Z. Q.; Chai, Z. F.; Shi, W. Q., Silver Ion-Mediated Heterometallic Three-Fold Interpenetrating Uranyl Organic Framework. *Inorg. Chem.* **2015,** *54*, 10934-10945.
[25] Chen, W.; Yuan, H. M.; Wang, J. Y.; Liu, Z. Y.; Xu, J. J.; Yang, M.; Chen, J. S., Synthesis, Structure, and Photoelectronic Effects of a Uranium-Zinc-Organic Coordination Polymer Containing Infinite Metal Oxide Sheets. *J. Am. Chem. Soc.* **2003,** *125*, 9266-9267.
[26] Mei, L.; Xie, Z. N.; Hu, K. Q.; Wang, L.; Yuan, L. Y.; Li, Z. J.; Chai, Z. F.; Shi, W. Q., First Three-Dimensional Actinide Polyrotaxane Framework Mediated by Windmill-like Six-Connected Oligomeric Uranyl: Dual Roles of the Pseudorotaxane Precursor. *Dalton Trans.* **2016,** *45*, 13304-13307.
[27] Thuery, P., Uranyl Ion Complexes with Cucurbit[5]uril: from Molecular Capsules to Uranyl-Organic Frameworks. *Cryst. Growth Des.* **2009,** *9*, 1208-1215.
[28] Liao, Z. L.; Li, G. D.; Wei, X. A.; Yu, Y.; Chen, J. S., Construction of Three-Dimensional Uranyl-Organic Frameworks with Benzenetricarboxylate Ligands. *Eur. J. Inorg. Chem.* **2010**, 3780-3788.
[29] Wu, H. Y.; Wang, R. X.; Yang, W. T.; Chen, J. L.; Sun, Z. M.; Li, J.; Zhang, H. J., 3-Fold-Interpenetrated Uranium-Organic Frameworks: New Strategy for Rationally Constructing Three-Dimensional Uranyl Organic Materials. *Inorg. Chem.* **2012,** *51*, 3103-3107.
[30] Yang, W. T.; Wu, H. Y.; Wang, R. X.; Pan, Q. J.; Sun, Z. M.; Zhang, H. J., From 1D Chain to 3D Framework Uranyl Diphosphonates: Syntheses, Crystal Structures, and Selective Ion Exchange. *Inorg. Chem.* **2012,** *51*, 11458-11465.
[31] Thuery, P.; Harrowfield, J., Uranyl-Organic Frameworks with Polycarboxylates: Unusual Effects of a Coordinating Solvent. *Cryst. Growth Des.* **2014,** *14*, 1314-1323.

[32] Zhang, Y. J.; Karatchevtseva, I.; Bhadbhade, M.; Tran, T. T.; Aharonovich, I.; Fanna, D. J.; Shepherd, N. D.; Lu, K.; Li, F.; Lumpkin, G. R., Solvothermal synthesis of uranium(VI) phases with aromatic carboxylate ligands: A dinuclear complex with 4-hydroxybenzoic acid and a 3D framework with terephthalic acid. *J. Solid State Chem.* **2016,** *234*, 22-28.
[33] Carlucci, L.; Ciani, G.; Proserpio, D. M.; Mitina, T. G.; Blatov, V. A., Entangled Two-Dimensional Coordination Networks: A General Survey. *Chem. Rev.* **2014,** *114*, 7557-7580.
[34] Batten, S. R.; Robson, R., Interpenetrating Nets: Ordered, Periodic Entanglement. *Angew. Chem. Int. Ed.* **1998,** *37*, 1460-1494.
[35] Carlucci, L.; Ciani, G.; Proserpio, D. M., Polycatenation, Polythreading and Polyknotting in Coordination Network Chemistry. *Coord. Chem. Rev.* **2003,** *246*, 247-289.
[36] Proserpio, D. M., Topological Crystal Chemistry Polycatenation Weaves a 3d Web. *Nature Chemistry* **2010,** *2*, 435-436.
[37] Thangavelu, S. G.; Butcher, R. J.; Cahill, C. L., Role of N-Donor Sterics on the Coordination Environment and Dimensionality of Uranyl Thiophenedicarboxylate Coordination Polymers. *Cryst. Growth Des.* **2015,** *15*, 3481-3492.
[38] Chen, F.; Wang, C. Z.; Li, Z. J.; Lan, J. H.; Ji, Y. Q.; Chai, Z. F., New Three-Fold Interpenetrated Uranyl Organic Framework Constructed by Terephthalic Acid and Imidazole Derivative. *Inorg. Chem.* **2015,** *54*, 3829-3834.
[39] Go, Y. B.; Wang, X. Q.; Jacobson, A. J., (6,3)-honeycomb structures of Uranium(VI) benzenedicarboxylate derivatives: The use of noncovalent interactions to prevent interpenetration. *Inorg. Chem.* **2007,** *46*, 6594-6600.
[40] Liu, C.; Gao, C. Y.; Yang, W. T.; Chen, F. Y.; Pan, Q. J.; Li, J. Y.; Sun, Z. M., Entangled Uranyl Organic Frameworks with (10,3)-b Topology and Polythreading Network: Structure, Luminescence, and Computational Investigation. *Inorg. Chem.* **2016,** *55*, 5540-5548.
[41] Zhao, R.; Mei, L.; Wang, L.; Chai, Z. F.; Shi, W. Q., Copper/Zinc-Directed Heterometallic Uranyl-Organic Polycatenating Frameworks: Synthesis, Characterization, and Anion-Dependent Structural Regulation. *Inorg. Chem.* **2016,** *55*, 10125-10134.
[42] Borkowski, L. A.; Cahill, C. L., Crystal Engineering with the Uranyl Cation II. Mixed Aliphatic Carboxylate/Aromatic Pyridyl Coordination Polymers: Synthesis, Crystal Structures, and Sensitized Luminescence. *Cryst. Growth Des.* **2006,** *6*, 2248-2259.
[43] Wang, Y. L.; Liu, Z. Y.; Li, Y. X.; Bai, Z. L.; Liu, W.; Wang, Y. X.; Xu, X. M.; Xiao, C. L.; Sheng, D. P.; Juan, D. W.; Su, J.; Chai, Z. F.; Albrecht-Schmitt, T. E.; Wang, S., Umbellate Distortions of the Uranyl Coordination Environment Result in a Stable and Porous Polycatenated Framework That Can Effectively Remove Cesium from Aqueous Solutions. *J. Am. Chem. Soc.* **2015,** *137*, 6144-6147.
[44] Thuery, P.; Harrowfield, J., Structural Variations in the Uranyl/4,4 '-Biphenyldicarboxylate System. Rare Examples of 2D -> 3D Polycatenated Uranyl-Organic Networks. *Inorg. Chem.* **2015,** *54*, 8093-8102.
[45] Thuery, P.; Harrowfield, J., Counter-ion control of structure in uranyl ion complexes with 2,5-thiophenedicarboxylate. *Crystengcomm* **2016,** *18*, 1550-1562.
[46] Thuery, P.; Riviere, E.; Harrowfield, J., Counterion-lnduced Variations in the Dimensionality and Topology of Uranyl Pimelate Complexes. *Cryst. Growth Des.* **2016,** *16*, 2826-2835.
[47] Thuery, P., From Helicates to Borromean Links: Chain Length Effect in Uranyl Ion Complexes of Aliphatic alpha,omega-Dicarboxylates. *Cryst. Growth Des.* **2016,** *16*, 546-549.

[48] Yu, Z. T.; Liao, Z. L.; Jiang, Y. S.; Li, G. H.; Chen, J. S., Water-insoluble Ag-U-organic assemblies with photocatalytic activity. *Chem. Eur. J.* **2005,** *11*, 2642-2650.
[49] Thangavelu, S. G.; Cahill, C. L., A Family of Uranyl Coordination Polymers Containing O-Donor Dicarboxylates and Trispyridyltriazine Guests. *Cryst. Growth Des.* **2016,** *16*, 42-50.
[50] Thangavelu, S. G.; Pope, S. J. A.; Cahill, C. L., Synthetic, structural, and luminescence study of uranyl coordination polymers containing chelating terpyridine and trispyridyltriazine ligands. *Crystengcomm* **2015,** *17*, 6236-6247.
[51] Gao, X.; Wang, C.; Shi, Z. F.; Song, J.; Bai, F. Y.; Wang, J. X.; Xing, Y. H., A family of uranyl-aromatic dicarboxylate (pht-, ipa-, tpa-) framework hybrid materials: photoluminescence, surface photovoltage and dye adsorption. *Dalton Trans.* **2015,** *44*, 11562-11571.
[52] Li, H. H.; Zeng, X. H.; Wu, H. Y.; Jie, X.; Zheng, S. T.; Chen, Z. R., Incorporating Guest Molecules into Honeycomb Structures Constructed from Uranium(VI)-Polycarboxylates: Structural Diversities and Photocatalytic Activities for the Degradation of Organic Dye. *Cryst. Growth Des.* **2015,** *15*, 10-13.
[53] Thangavelu, S. G.; Andrews, M. B.; Pope, S. J. A.; Cahill, C. L., Synthesis, Structures, and Luminescent Properties of Uranyl Terpyridine Aromatic Carboxylate Coordination Polymers. *Inorg. Chem.* **2013,** *52*, 2060-2069.
[54] Knope, K. E.; de Lill, D. T.; Rowland, C. E.; Cantos, P. M.; de Bettencourt-Dias, A.; Cahill, C. L., Uranyl Sensitization of Samarium(III) Luminescence in a Two-Dimensional Coordination Polymer. *Inorg. Chem.* **2012,** *51*, 201-206.
[55] Dolomanov, O. V.; Bourhis, L. J.; Gildea, R. J.; Howard, J. A. K.; Puschmann, H., OLEX2: a complete structure solution, refinement and analysis program. *J. Appl. Crystallogr.* **2009,** *42*, 339-341.
[56] Sheldrick, G. M., A short history of SHELX. *Acta Crystallogr. A* **2008,** *64*, 112-122.
[57] Sheldrick, G. M., SHELXT - Integrated space-group and crystal-structure determination. *Acta Crystallogr. A* **2015,** *71*, 3-8.
[58] Spek, A. L., Structure validation in chemical crystallography. *Acta Crystallogr. D* **2009,** *65*, 148-155.
[59] Spek, A., The Extended PLATON/SQUEEZE Tool in the Context of Twinning and SHELXL2014. *Acta Crystallogr. A* **2014,** *70*, C1436.
[60] Frisch, M. J.; Trucks, G. W.; Schlegel, H. B.; Scuseria, G. E.; Robb, M. A.; Cheeseman, J. R.; Scalmani, G.; Barone, V.; Mennucci, B.; Petersson, G. A.; Nakatsuji, H.; Caricato, M.; Li, X.; Hratchian, H. P.; Izmaylov, A. F.; Bloino, J.; Zheng, G.; Sonnenberg, J. L.; Hada, M.; Ehara, M.; Toyota, K.; Fukuda, R.; Hasegawa, J.; Ishida, M.; Nakajima, T.; Honda, Y.; Kitao, O.; Nakai, H.; Vreven, T.; Montgomery Jr., J. A.; Peralta, J. E.; Ogliaro, F.; Bearpark, M. J.; Heyd, J.; Brothers, E. N.; Kudin, K. N.; Staroverov, V. N.; Kobayashi, R.; Normand, J.; Raghavachari, K.; Rendell, A. P.; Burant, J. C.; Iyengar, S. S.; Tomasi, J.; Cossi, M.; Rega, N.; Millam, N. J.; Klene, M.; Knox, J. E.; Cross, J. B.; Bakken, V.; Adamo, C.; Jaramillo, J.; Gomperts, R.; Stratmann, R. E.; Yazyev, O.; Austin, A. J.; Cammi, R.; Pomelli, C.; Ochterski, J. W.; Martin, R. L.; Morokuma, K.; Zakrzewski, V. G.; Voth, G. A.; Salvador, P.; Dannenberg, J. J.; Dapprich, S.; Daniels, A. D.; Farkas, Ö.; Foresman, J. B.; Ortiz, J. V.; Cioslowski, J.; Fox, D. J. *Gaussian 09 Revision A.02*, Gaussian, Inc.: Wallingford, CT, USA, 2009.
[61] Lee, C. T.; Yang, W. T.; Parr, R. G., Development Of the Colle-Salvetti Correlation-Energy Formula into a Functional Of the Electron-Density. *Phys. Rev. B.* **1988,** *37*, 785-789.
[62] Becke, A. D., Density-Functional Thermochemistry. 3. The Role Of Exact Exchange. *J. Chem. Phys.* **1993,** *98*, 5648-5652.

[63] Dolg, M.; Stoll, H.; Preuss, H., Energy-Adjusted Abinitio Pseudopotentials for the Rare-Earth Elements. *J. Chem. Phys.* **1989,** *90*, 1730-1734.
[64] Küchle, W.; Dolg, M.; Stoll, H.; Preuss, H., Energy‐Adjusted Pseudopotentials for the Actinides. Parameter Sets and Test Calculations for Thorium and Thorium Monoxide. *J. Chem. Phys.* **1994,** *100*, 7535-7542.
[65] Cao, X.; Dolg, M., Segmented Contraction Scheme for Small-Core Actinide Pseudopotential Basis Sets. *J. Mol. Struc.-Theochem* **2004,** *673*, 203-209.
[66] Reed, A. E.; Curtiss, L. A.; Weinhold, F., Intermolecular Interactions From a Natural Bond Orbital, Donor-Acceptor Viewpoint. *Chem. Rev.* **1988,** *88*, 899-926.
[67] Kerr, A. T.; Cahill, C. L., Crystal Engineering with the Uranyl Cation Ill. Mixed Aliphatic Dicarboxylate/Aromatic Dipyridyl Coordination Polymers: Synthesis, Structures, and Speciation. *Cryst. Growth Des.* **2011,** *11*, 5634-5641.
[68] Denning, R. G., Electronic structure and bonding in actinyl ions and their analogs. *J. Phys. Chem. A* **2007,** *111*, 4125-4143.
[69] Natrajan, L. S., Developments in the photophysics and photochemistry of actinide ions and their coordination compounds. *Coord. Chem. Rev.* **2012,** *256*, 1583-1603.
[70] Thuery, P.; Harrowfield, J., Solvent Effects in Solvo-Hydrothermal Synthesis of Uranyl Ion Complexes with 1,3-Adamantanediacetate. *Crystengcomm* **2015,** *17*, 4006-4018.
[71] Thuery, P.; Riviere, E.; Harrowfield, J., Uranyl and Uranyl-3d Block Cation Complexes with 1,3-Adamantanedicarboxylate: Crystal Structures, Luminescence, and Magnetic Properties. *Inorg. Chem.* **2015,** *54*, 2838-2850.
[72] Brachmann, A.; Geipel, G.; Bernhard, G.; Nitsche, H., Study of Uranyl(VI) Malonate Complexation by Time Resolved Laser-Induced Fluorescence Spectroscopy (TRLFS). *Radiochim. Acta* **2002,** *90*, 147-153.
[73] Borkowski, L. A.; Cahill, C. L., Topological evolution in uranyl dicarboxylates: Synthesis and structures of one-dimensional UO2(C6H8O4)(H2O)(2) and three-dimensional UO2(C6H8O4). *Inorg. Chem.* **2003,** *42*, 7041-7045.
[74] Borkowski, L. A.; Cahill, C. L., Crystal engineering with the uranyl cation I. Aliphatic carboxylate coordination polymers: Synthesis, crystal structures, and fluorescent properties. *Cryst. Growth Des.* **2006,** *6*, 2241-2247.
[75] Borkowski, L. A.; Cahill, C. L., A novel uranium-containing coordination polymer: poly[dioxouranium(VI)-mu(4)-n-pentane-1,5-dicarboxylato]. *Acta Crystallogr. E* **2005,** *61*, M816-M817.

Table of Contents Graphic and Synopsis

Synopsis：

A series of novel uranyl terephthalate polycatenated frameworks has been synthesized from uranyl nitrate and terephthalic acid through a templated-synthesis method using organic bases, 1,3-(4,4‘-bispyridyl)propane (BPP) or 4,4‘-bipyridine (BPY) for the first time. The vital role of organic base as the template agent has been demonstrated by a direct comparison between these polycatenated frameworks and previously reported uranyl terephthalate compounds, as well as by DFT calculations.